

Fluorescent imidazolium receptors for the recognition of pyrophosphate

Sook Kyung Kim,^a N. Jiten Singh,^b Jiyoung Kwon,^a In-Chul Hwang,^b Su Jin Park,^a
Kwang S. Kim^{b,*} and Juyoung Yoon^{a,*}

^aDepartment of Chemistry and Division of Nano Science, Ewha Womans University, 11-1 Daehyon-Dong,
Sodaemun-Ku, Seoul 120-750, Republic of Korea

^bNational Creative Research Initiative Center for Superfunctional Materials, Department of Chemistry, Division of Molecular and Life
Sciences, Pohang University of Science and Technology, San 31, Hyojadong, Namgu, Pohang 790-784, Republic of Korea

Received 6 February 2006; revised 30 March 2006; accepted 31 March 2006
Available online 2 May 2006

Abstract—Anthracene and binaphthyl derivatives bearing two imidazolium rings, which strongly bind anions and are particularly selective for pyrophosphate, are examined using fluorescence, ¹H NMR analysis, and density functional calculations.
© 2006 Elsevier Ltd. All rights reserved.

1. Introduction

Anions play an important role in a wide range of chemical and biological processes, and numerous efforts have been devoted to the development of abiotic receptors for anionic species.¹ Sensors based on anion-induced changes in fluorescence appear to be particularly attractive due to the simplicity and high detection limit of fluorescence.^{1f,2} Particularly, pyrophosphate can be a biologically important target since it is the product of ATP hydrolysis under cellular conditions.³ However, there have been only a few reports regarding pyrophosphate selective receptors using the fluorescent changes as the means of detection.⁴

In contrast to the well-known type of hydrogen bonding for the anion binding such as amide, pyrrole, urea, etc., various types of receptors containing imidazolium moieties,⁵ such as the benzene-based tripodal imidazolium receptors,⁶ imidazolium cyclophanes,⁷ calix[*n*]imidazolium,⁸ imidazolium anthracenes,⁹ imidazolium calix[4]arene,¹⁰ imidazolium cavitand,¹¹ and imidazolium polythiophene¹² have been reported. Especially, we have recently reported a fluorescent anthracene derivative bearing two imidazolium moieties on its 1,8-positions (**1**) (Fig. 1), which shows selective binding for H₂PO₄[−] over other anions when the anions are monitored individually.^{9b} We have further demonstrated that the selectivity of these imidazolium receptors against anions can be

controlled by the topology of the binding site (e.g., enhancement of rigidity).^{9c} Compared to the host **1**, the more rigidity in host **2** enhances the binding selectivity for H₂PO₄[−] over F[−].^{9c} In both cases, anthracene being fluorophore has the advantage of being considered as rigid templates in terms of sensing anions by the change in the fluorophore intensity due to photo-induced electron transfer (PET) mechanism.

In an effort to understand the conceptual design of this class of anion sensors, we have further synthesized two new fluorescent chemosensors by the diversification of the frame and investigated more in details for its anion binding properties. Herein, we report two new fluorescent anion receptors (**3** and **4**) bearing two imidazolium groups at the 9,10-positions of anthracene and 2,2'-positions of binaphthyl ring, respectively. The crystal structure of **3** is also reported. The binding properties of these new host systems toward various anions including HP₂O₇^{3−} and H₂PO₄[−] were examined using fluorescence. Two known systems (**1** and **2**) were reinvestigated for the binding affinity toward pyrophosphate. We also carried out theoretical investigation in order to understand the binding mode of the anions with these receptors. Host (**S**)-**4** shows a unique selectivity for HP₂O₇^{3−}, which is simply induced from two imidazolium groups immobilized on a binaphthyl moiety. Furthermore, the binding property of hosts **3** and **4** toward various anions was compared with that of hosts **1** and **2**. We notice that **2** has the highest binding affinity and selectivity toward HP₂O₇^{3−} via ion-pairing interaction mode against the conventional ionic–hydrogen bonding of anions with the imidazolium based receptors. Finally, we briefly describe the relationship between the receptor structure and anion binding strength.

* Corresponding authors. Tel.: +82 54 279 2110; fax: +82 54 279 8137 (K.S.K.); tel.: +82 2 3277 2400; fax: +82 2 3277 2384 (J.Y.); e-mail addresses: kim@postech.ac.kr; jyoon@ewha.ac.kr

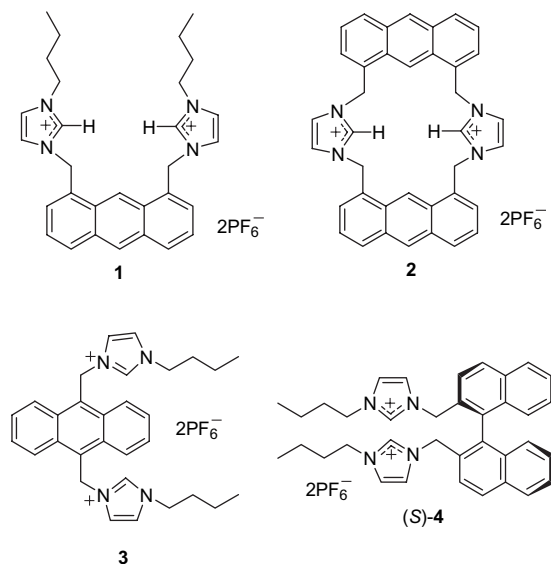
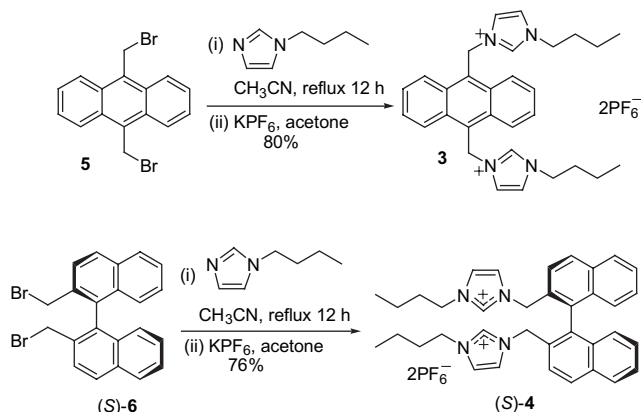


Figure 1. Structures of fluorescent imidazolium receptors.

2. Results and discussion

The synthetic procedures of compounds **3** and **4** are summarized in Scheme 1. Compounds **3** and **4** were synthesized by the reactions of 9,10-bis(bromomethyl)anthracene **5**^{4c} and (*S*)-(-)-2,2'-bis(bromomethyl)-1,1'-binaphthyl **6**¹² with 1-butylimidazole, respectively, in CH₃CN. The solvent was evaporated to dryness; 10 mL of acetone was added to the residue and stirred for 20 min at room temperature, followed by anion exchange with KPF₆. After another 24 h stirring at room temperature, the reaction mixture was filtered and the filtrate was evaporated. To the oily crude product, about 5 mL of ethyl acetate was added and precipitation occurred. The precipitate was then filtered and washed with CH₂Cl₂ to give analytically pure product.



Scheme 1. Synthesis of hosts **3** and **4**.

The X-ray crystal structural analysis of **3**·2[PF₆][−] revealed a 'trans' conformation of two butyl imidazolium groups on either side of anthracene moiety with C_{2v} inversion symmetry. The positively charged (C–H)⁺ imidazolium groups point individually toward the counter anions (PF₆)[−] (Fig. 2). Selected hydrogen interionic distances are *d*(H1⋯F4)=2.623 Å and *d*(H1⋯F3)=2.802 Å.

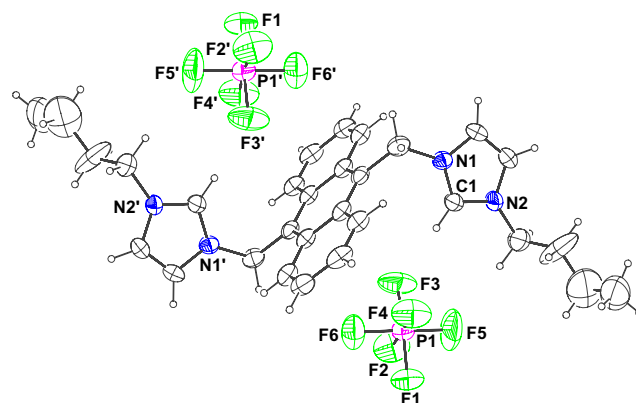


Figure 2. Crystal structure of **3**·2(PF₆)[−] (thermal ellipsoids set at 30% probability). Selected interionic distances: H1–F4=2.623 Å, H1–F3=2.802 Å.

The fluorescence emission changes of **3** upon the addition of HSO₄[−], CH₃CO₂[−], I[−], Br[−], Cl[−], F[−], H₂PO₄[−], and HP₂O₇^{3−} are illustrated in Figure 3. Among the anions examined, compound **3** displays strong fluorescent quenching effects with H₂PO₄[−] and HP₂O₇^{3−}. From the fluorescence titration experiments, the association constants for HP₂O₇^{3−} (Fig. 4), H₂PO₄[−], CH₃CO₂[−], Br[−], and I[−] are observed to be 3.58×10⁶, 6.31×10⁵, 7.30×10³, 2.87×10³, and 1.09×10³ M^{−1} (errors≤10%), respectively.¹⁴ As shown in Job's plot (Fig. 5), host **3** shows 1/1 binding with HP₂O₇^{3−} in acetonitrile. The change in Gibbs free energy for Br[−] as determined by the ¹H NMR titration is 4.1 kcal/mol, which is in good agreement with the fluorescence titration (4.7 kcal/mol). Host **3** shows selective binding with HP₂O₇^{3−} and H₂PO₄[−] ions over CH₃CO₂[−], F[−], Cl[−], and Br[−] ions (Table 1). We observed the ¹H NMR spectral change upon the addition of the anion as tetrabutylammonium salts in acetonitrile-*d*₃. Upon the addition of 1 equiv of Cl[−], Br[−], I[−], and HSO₄[−] to host **3**, downfield shifts (Δδ≅1.38, 1.12, 0.33, and 0.16, respectively) were observed for the C(2) proton of imidazolium moieties, clearly suggesting **3**·anion complexation by (C–H)⁺–anion ionic hydrogen bonds. However, in acetonitrile-*d*₃, addition of F[−] or H₂PO₄[−] to host **3** resulted in a precipitate.

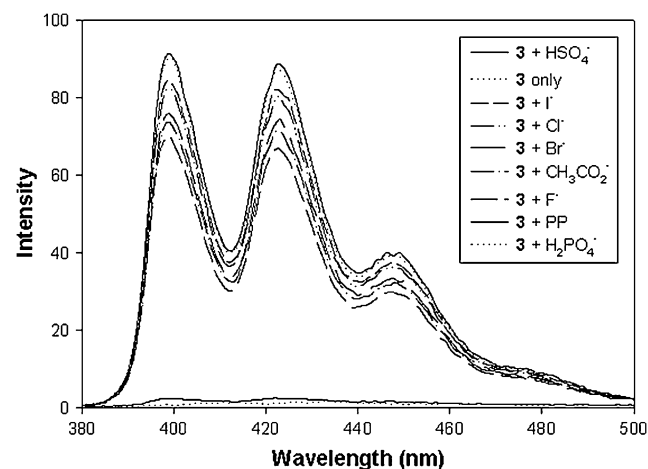


Figure 3. Fluorescent emission changes of **3** (6 μM) upon the addition of tetrabutylammonium salt of HSO₄[−], CH₃CO₂[−], I[−], Br[−], Cl[−], F[−], H₂PO₄[−], and HP₂O₇^{3−} (10 equiv) in acetonitrile (excitation at 365 nm) (excitation and emission slit: 3 nm).

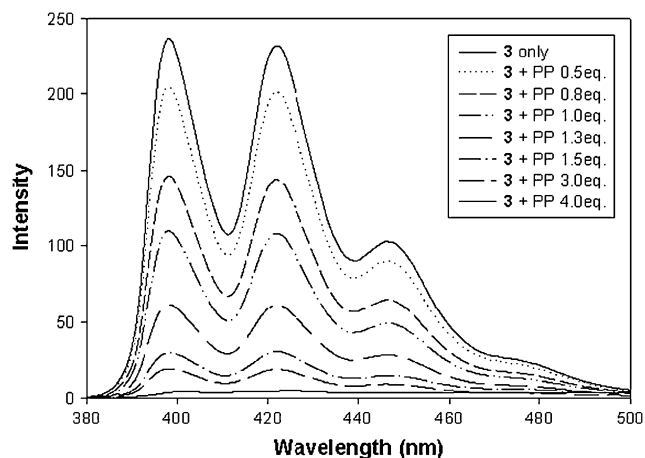


Figure 4. Fluorescent titrations of compound **3** (1 μ M) with tris(tetrabutylammonium) hydrogenpyrophosphate in acetonitrile (excitation at 365 nm) (excitation and emission slit: 5 nm).

There are quite a few papers regarding fluorescent chemosensors for anions bearing benzylic amine^{1f,4g} or urea groups,^{1f,2,4a,c} which are based on photo-induced electron transfer (PET) mechanism. However, only a few fluorescent signaling systems bearing imidazolium groups for anions have been reported.^{9b,c,11b,15} Our anthracene and binaphthalene based receptors (**1–4**) should in principle show also ideal PET behavior upon anion recognition. As shown in Figure 3, H_2PO_4^- and $\text{HP}_2\text{O}_7^{3-}$ quenched the emission effectively ($\sim 95\%$); on the other hand, no other spectral changes were observed in the emission spectra, i.e., there was no evidence of either exciplex or excimer emission. Furthermore, the changes in the absorption spectra of anthracene moiety were negligible. Since the binding sites of these receptors are separated from the fluorophore via methylene spacer, the observations are consistent with the typical PET behavior.

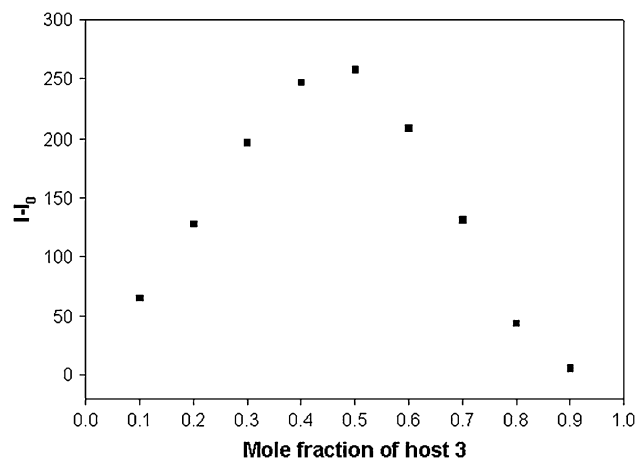


Figure 5. Job's plot of compound **3** (1 μ M) with tris(tetrabutylammonium) hydrogenpyrophosphate in acetonitrile using its fluorescent changes (excitation at 365 nm and emission at 422 nm) (excitation and emission slit: 5 nm).

Figure 6 shows fluorescent emission changes of **4** (6 μ M) upon the addition of tetrabutylammonium salt of HSO_4^- , CH_3CO_2^- , I^- , Br^- , Cl^- , F^- , H_2PO_4^- , and $\text{HP}_2\text{O}_7^{3-}$ (10 equiv) in acetonitrile, while Figure 7 shows the fluorescence titration experiments of host **4** with $\text{HP}_2\text{O}_7^{3-}$. As shown in Table 1, from the fluorescence titration, the association constants for $\text{HP}_2\text{O}_7^{3-}$, H_2PO_4^- , CH_3CO_2^- , F^- , Cl^- , Br^- , and I^- are observed to be 6.76×10^6 , 4.21×10^5 , 1.26×10^5 , 4.09×10^5 , 2.78×10^3 , 1.87×10^3 , and $1.14 \times 10^3 \text{ M}^{-1}$ (errors $\leq 10\%$), respectively.¹³ The selectivity for $\text{HP}_2\text{O}_7^{3-}$ is about 12 times greater than H_2PO_4^- and F^- .

Among the series of hosts (**1–4**) examined, a dimer host (**2**) displays a largest binding constant with $\text{HP}_2\text{O}_7^{3-}$ (Fig. 8), which indicates that the preorganized rigid binding pocket may play an important role in the binding with $\text{HP}_2\text{O}_7^{3-}$.

Table 1. Calculated interaction energies and experimental free energy changes for host–anion complexes in kcal/mol^a

Host	Anion	$K_a \text{ (M}^{-1}\text{)}^a$	$-\Delta G_{\text{expt}}$	$-\Delta E_{\text{calcd}}^{\text{gas}}$	$-\Delta E_{\text{calcd}}^{\text{MeCN}}$	$-\Delta G^{\text{scaled}}$
1	$\text{HP}_2\text{PO}_7^{3-}$	5.43×10^6	9.18	482.11	15.44	10.04
	H_2PO_4^-	$\sim 1.30 \times 10^6$	~ 8.34	165.50	13.45	8.74
	Cl^-	7900	5.31	—	—	—
	Br^-	4500	4.98	—	—	—
2	$\text{HP}_2\text{PO}_7^{3-}$	$\sim 1.01 \times 10^8$	~ 10.91	484.50	17.60 (11.53)	11.44 (7.49)
	H_2PO_4^-	$\sim 1.30 \times 10^6$	~ 8.34	169.49	12.76	8.29
	F^-	340,000	7.54	179.71	11.44	7.43
	Cl^-	2000	4.49	—	—	—
	Br^-	780	3.94	—	—	—
3	$\text{HP}_2\text{PO}_7^{3-}$	3.58×10^6	8.93	469.36	11.06	7.19
	H_2PO_4^-	631,000	7.91	164.59	10.57	6.87
	CH_3COO^-	7300	5.27	167.87	9.46	6.15
	Br^-	2870	4.71	—	—	—
4	$\text{HP}_2\text{PO}_7^{3-}$	6.76×10^6	9.31	471.90	15.81	9.48
	H_2PO_4^-	421,000	7.67	155.50	13.04	7.82
	CH_3COO^-	126,000	6.95	163.46	11.39	6.84
	F^-	409,000	7.65	173.49	12.04	7.23
	Cl^-	2780	4.69	—	—	—
	Br^-	1870	4.46	—	—	—

^a The association constants $K_a \text{ (M}^{-1}\text{)}$ were measured using the fluorescence titration. ΔG_{expt} are the changes in Gibbs' free energy in acetonitrile solution measured by fluorescence titration. Anions used are in the form of tetrabutylammonium salts. $\Delta E_{\text{calcd}}^{\text{gas}}$ is the interaction energy in the gas phase at the B3LYP/6-31(+)G* level of theory. $\Delta E_{\text{calcd}}^{\text{soln}} = \Delta E_{\text{H-anion}}^{\text{soln}} - \Delta E_{\text{soln-anion}}^{\text{soln}}$, where $\Delta E_{\text{H-anion}}^{\text{soln}}$ is the interaction energy of the H–anion complex (H=**1–4**) in acetonitrile solution based on isodensity surface polarized continuum model (IPCM). $\Delta E_{\text{soln-anion}}^{\text{soln}}$ is the interaction energy of the anion with solvent molecules in the first solvation shell of an anion. The free energy change (ΔG_{scaled}) was approximately obtained by scaling (65%) the internal energy change to fit to the experimental value.

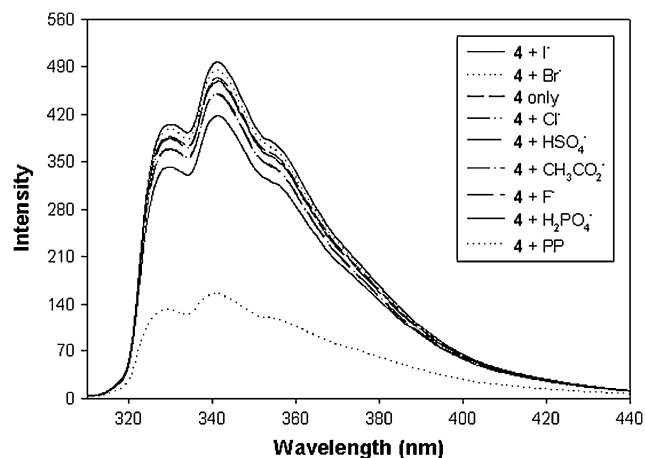


Figure 6. Fluorescent emission changes of **4** (6 μ M) upon the addition of tetrabutylammonium salt of HSO_4^- , CH_3CO_2^- , I^- , Br^- , Cl^- , F^- , H_2PO_4^- , and hydrogenpyrophosphate (10 equiv) in acetonitrile (excitation at 310 nm) (excitation and emission slit: 3 nm).

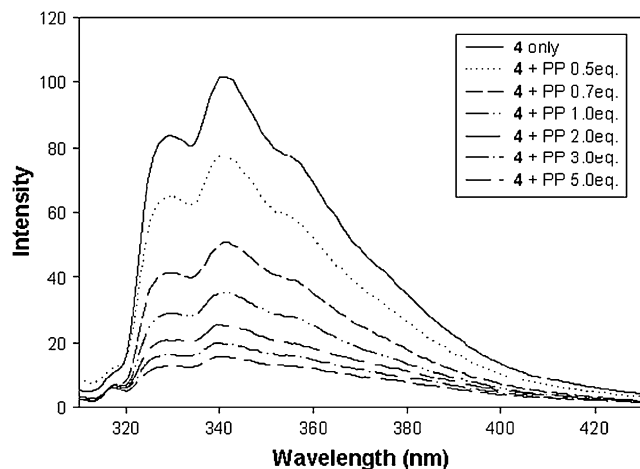


Figure 7. Fluorescent titrations of compound **4** (1 μ M) with tris(tetrabutylammonium) hydrogenpyrophosphate in acetonitrile (excitation at 310 nm) (excitation and emission slit: 3 nm).

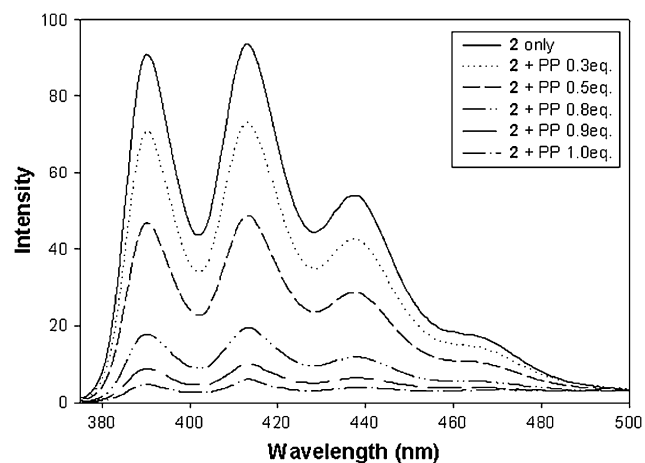


Figure 8. Fluorescent titrations of compound **2** (1 μ M) with tris(tetrabutylammonium) hydrogenpyrophosphate in acetonitrile (excitation at 365 nm) (excitation and emission slit: 3 nm).

The binding constants of **1–4** with $\text{HP}_2\text{O}_7^{3-}$ are in the order of $2 > 4 \cong 1 > 3$, which is consistent with our assumption.

The competitive binding studies of hosts **2** and **4** with respect to $\text{HP}_2\text{O}_7^{3-}$ using fluorescent changes clearly show that host **2** binds more tightly with $\text{HP}_2\text{O}_7^{3-}$ than **4** does. As shown in Figure 9, the fluorescent intensity of host **4** was almost recovered when host **2** was added to the solution of host **4** and $\text{HP}_2\text{O}_7^{3-}$, and the fluorescent intensity of host **2** was quenched quite significantly.

From ^1H NMR it is observed that upon the addition of $\text{HP}_2\text{O}_7^{3-}$ (0.5 equiv) to the solution of **4** in acetonitrile, both imidazolium C-2 hydrogen peaks (8.53 ppm) moved to 9.66 ppm with severe broadness. And they disappear even at the low concentration of guest (1 equiv) possibly due to the transfer of hydrogen atom from the imidazolium moieties to $\text{HP}_2\text{O}_7^{3-}$ (Fig. 10). Also, one of the benzyl hydrogens displays large downfield shift (~ 1 ppm) when $\text{HP}_2\text{O}_7^{3-}$ was added. On the contrary, imidazolium C-2 hydrogens of host **4** display only downfield shifts (~ 1 ppm) upon the addition of H_2PO_4^- and one of the benzyl hydrogens displays less downfield shift (< 0.5 ppm) compared to that with $\text{HP}_2\text{O}_7^{3-}$ (Fig. 11). Similar proton transfer was also observed in ^1H NMR spectra of host **3** when $\text{HP}_2\text{O}_7^{3-}$ was added in $\text{DMSO}-d_6$ at room temperature. Similar broadness of the imidazolium C-2 hydrogens as well as a downfield shift (9.09–9.54 ppm) of these protons was observed, while there was only small downfield (~ 0.3 ppm; 6.56–6.86 ppm) in the benzyl protons.

The thermodynamic origin of the cooperativity of ion-pairing in molecular recognition was investigated with the positively charged anion receptors containing ammonium groups.¹⁶ On the other hand, imidazolium based receptors have strong tendency to form ionic hydrogen bonding with anions, which is explained by the ^1H NMR chemical shift of the imidazolium C-2 hydrogen. However, the observation of no chemical shift between some of the receptors studied here upon the addition of H_2PO_4^- and $\text{HP}_2\text{O}_7^{3-}$ has questioned about the nature of interaction between host and guest. Therefore, the theoretical investigation¹⁷ for the most stable conformer of host–guest complex is essential in order to

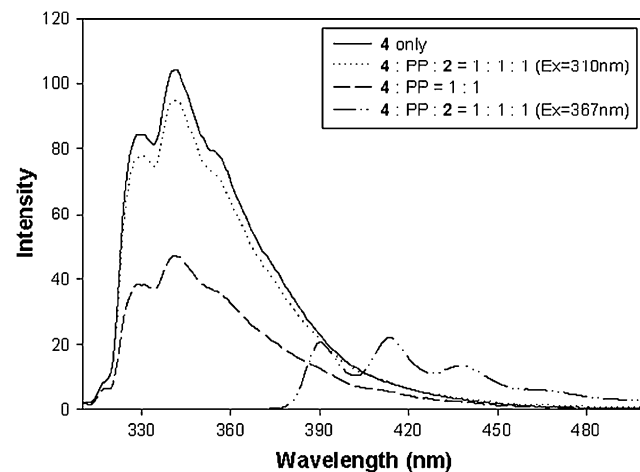


Figure 9. Competitive binding studies of **2** (1 μ M) and **4** (1 μ M) with $\text{HP}_2\text{O}_7^{3-}$ (1 equiv) in acetonitrile (excitation at 310 or 367 nm) (excitation and emission slit: 3 nm).

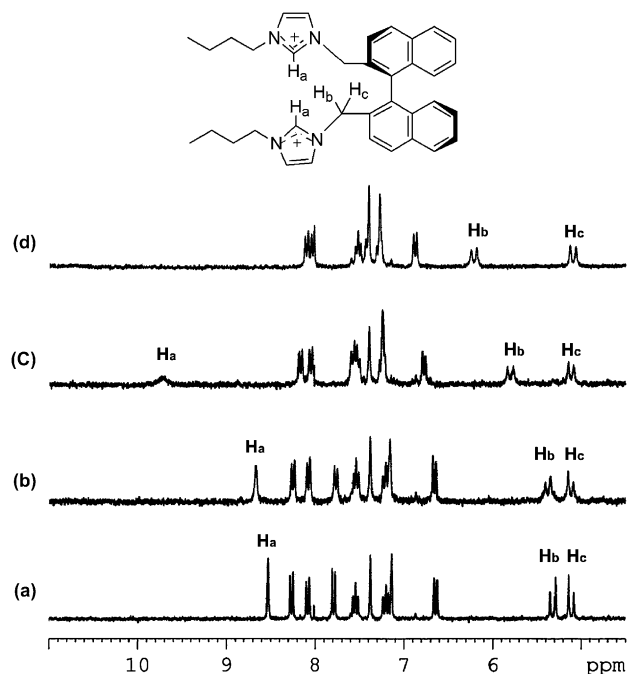


Figure 10. Partial ^1H NMR (250 MHz) of **4** (2 mM) in $\text{DMSO}-d_6$. (a) Compound **4** only; (b) **4**+0.2 equiv of tris(tetrabutylammonium) hydrogenpyrophosphate; (c) **4**+0.5 equiv of tris(tetrabutylammonium) hydrogenpyrophosphate; (d) **4**+1 equiv of tris(tetrabutylammonium) hydrogenpyrophosphate.

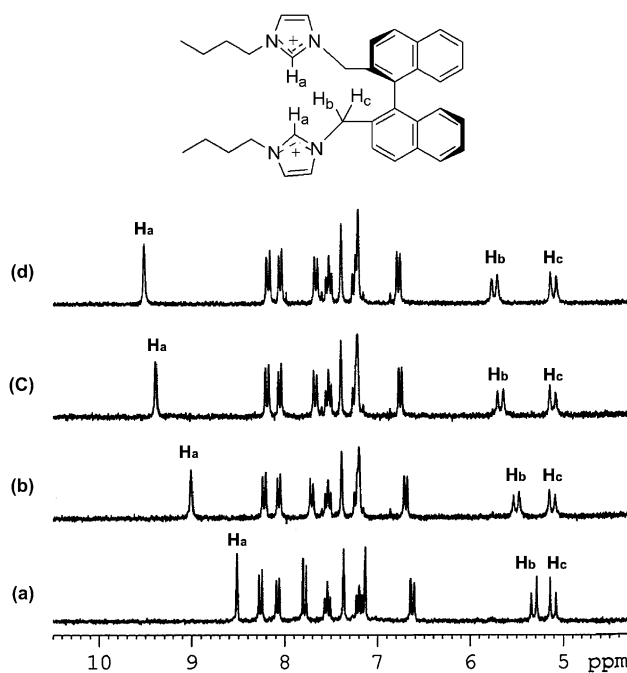


Figure 11. Partial ^1H NMR (250 MHz) of **4** (2 mM) in $\text{DMSO}-d_6$. (a) Compound **4** only; (b) **4**+1.5 equiv of tetrabutylammonium dihydrogenphosphate; (c) **4**+3 equiv of tetrabutylammonium dihydrogenphosphate; (d) **4**+5 equiv of tetrabutylammonium dihydrogenphosphate.

understand the nature of binding interaction. At the optimized geometries of **3** and **4** with $\text{HP}_2\text{O}_7^{3-}$ we note that one of the imidazolium C-2 hydrogen has been completely transferred to the $\text{HP}_2\text{O}_7^{3-}$ (Fig. 12) as observed in ^1H NMR titration. In the optimized geometry of **1** with $\text{HP}_2\text{O}_7^{3-}$, we do not

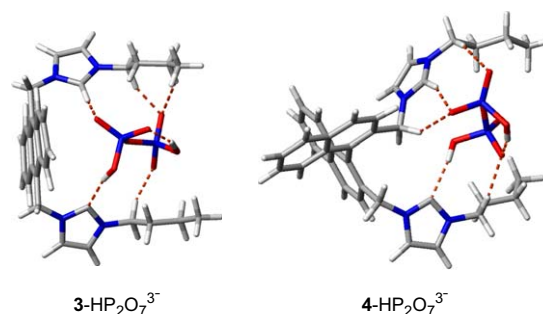


Figure 12. Optimized geometry of (a) $3\cdot\text{HP}_2\text{O}_7^{3-}$ and (b) $4\cdot\text{HP}_2\text{O}_7^{3-}$ complexes. Dotted lines show distances less than 2.5 Å.

see any proton transfer unlike the cases of **3** and **4** with $\text{HP}_2\text{O}_7^{3-}$. In a while, the optimized geometry of **2** with $\text{HP}_2\text{O}_7^{3-}$ shows two distinct modes of interactions between host and guest. In one mode one of the imidazolium C-2 hydrogen has been completely transferred to $\text{HP}_2\text{O}_7^{3-}$. In the other mode the interaction between **2** and $\text{HP}_2\text{O}_7^{3-}$ surprised us as it forms a complex where the major interaction between host and guest is the ion-pair interaction, thereby the orientation of the oxygen atoms of $\text{HP}_2\text{O}_7^{3-}$ is not properly angled for the maximal H-bonding with the imidazolium C-2 hydrogen atoms. Both the bonding modes show nearly the same binding energy in the gas phase, which is higher than other anions by at least ~ 300 kcal/mol. However, in acetonitrile the ion-pair complex conformer is found to be 6 kcal/mol more stable than the complex formed by proton transfer. Similarly, the most stable conformer for $1\cdot\text{HP}_2\text{O}_7^{3-}$ is the ion-pair complex. The ^1H NMR titration of **1** and **2** with $\text{HP}_2\text{O}_7^{3-}$ in DMSO shows that there is no chemical shift of imidazolium C-2 hydrogen at the molar ratio of 0.1–0.3 equiv of $\text{HP}_2\text{O}_7^{3-}$; the solution starts precipitating upon the addition of ~ 0.5 equiv of $\text{HP}_2\text{O}_7^{3-}$. This experimental finding also supports our prediction of ion-pair interaction mode between **1/2** and $\text{HP}_2\text{O}_7^{3-}$.

Table 1 illustrates the ab initio calculation results for host–anion complexes. In the gas phase, the binding energy of host **3** with $\text{HP}_2\text{O}_7^{3-}$ is much larger than other anions by at least ~ 300 kcal/mol. Since ionic hydrogen bond strength is dependent on solvent polarity and interaction of the anion with the solvent molecules, the binding energies are much lowered in polar solvents.¹⁸ Therefore, in acetonitrile, the binding energy gain of host **3** in favor of $\text{HP}_2\text{O}_7^{3-}$ is 0.3 and 1.0 kcal/mol for H_2PO_4^- and CH_3CO_2^- , respectively. The binding energies of **4** with $\text{HP}_2\text{O}_7^{3-}$ in the gas phase are larger than that of H_2PO_4^- , CH_3CO_2^- , and F^- by 316, 308, and 298 kcal/mol, respectively (Table 1). Therefore, in acetonitrile, the binding energy gain of host **4** is in favor of $\text{HP}_2\text{O}_7^{3-}$ over H_2PO_4^- , CH_3CO_2^- , and F^- by 1.7, 2.6, and 2.3 kcal/mol, respectively.

Meanwhile, the binding energies in acetonitrile of host **1** and **2** with $\text{HP}_2\text{O}_7^{3-}$ in the gas phase were predicted to be at least ~ 300 kcal/mol more than other anions, whereas in acetonitrile the binding energy **1/2** with $\text{HP}_2\text{O}_7^{3-}$ is larger than that of H_2PO_4^- by 1.3/3.1 kcal/mol.

The average Mulliken atomic charges (B3LYP/6-31G*) on the oxygen atoms of $\text{HP}_2\text{O}_7^{3-}$ is -0.79 . The same for H_2PO_4^- and CH_3CO_2^- are -0.67 and -0.64 , respectively.

Just by considering the columbic interaction between the cationic divalent receptors (**1–4**) and non-spherical anions the trivalent anionic species $\text{HP}_2\text{O}_7^{3-}$ will be more strongly interacting than the monovalent anionic species (H_2PO_4^- and CH_3CO_2^-). The binding affinity of H_2PO_4^- is expected to be higher than that of CH_3CO_2^- . All the receptors (**1–4**) obey the same trends. On the other hand, the open form of the receptors (**1**, **3**, and **4**) has lower binding affinity for $\text{HP}_2\text{O}_7^{3-}$ than the close form (**2**) despite the fact that all are divalent cationic receptors. The most stable conformers of **1** and **4** have two imidazolium arms in the form of tweezers, meanwhile **3**, in trans form (as in the crystal structure, Fig. 2). Therefore, in order to form the stable complex with anions, it needs to rearrange the binding arms at the cost of the entropy energy. Meanwhile, the energy lost due to entropy will be minimal in the case of **2** as it has rigid/pre-organized form of the binding arms. The combined effect of rigidity and ion-pair interactions leads **2** to have stronger binding affinity toward $\text{HP}_2\text{O}_7^{3-}$.

From the above experimental and theoretical investigations, we notice that all the dipodal receptors studied have more or at least equal binding affinity toward $\text{HP}_2\text{O}_7^{3-}$ or H_2PO_4^- against other anions. This suggests that this class of imidazolium dipodal receptors shows strong binding with the V-shaped and tetrahedral shaped anions, which prefers more directed H-bonding interaction. Anthracene was found to be the most appropriate size of the rigid frame in our model system for the maximal interaction between host and $\text{HP}_2\text{O}_7^{3-}$ (Fig. 13).

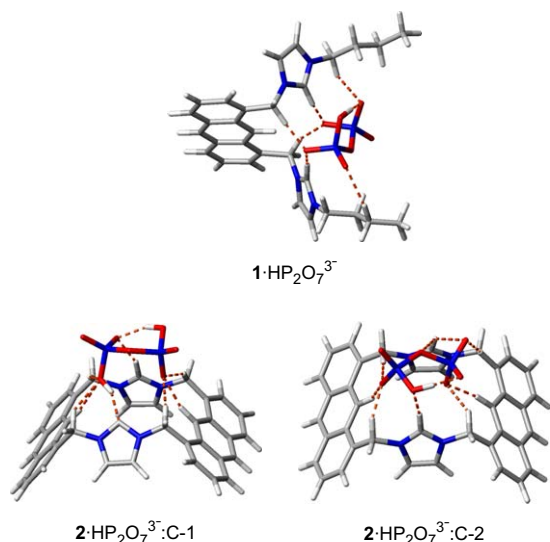


Figure 13. Optimized geometry of **1**· $\text{HP}_2\text{O}_7^{3-}$ and two conformers C-1 and C-2 of **2**· $\text{HP}_2\text{O}_7^{3-}$ complexes. Dotted lines show distances less than 2.5 Å.

3. Conclusion

Anthracene and binaphthyl derivatives bearing two imidazolium moieties were synthesized as fluorescent chemosensors for anions and investigated using fluorescence, ^1H NMR analysis, density functional calculations, and X-ray diffractometer analysis. The anthracene and binaphthalene based receptors display particularly selective binding for pyro-

phosphate and phosphate. Therefore, the selectivity of these imidazolium receptors against anions can be controlled by the topology of the binding site. The conceptual design approach adopted here could be applied to other imidazolium based receptors with diverse topological features.

4. Experimental

4.1. General methods

Unless otherwise noted, materials were obtained from commercial suppliers and were used without further purification. Flash chromatography was carried out on silica gel 60 (230–400 mesh ASTM; Merck). Thin layer chromatography (TLC) was carried out using Merck 60 F₂₅₄ plates with thickness of 0.25 mm. Preparative TLC was performed using Merck 60 F₂₅₄ plates with the thickness of 1 mm.

Melting points were measured using a Büchi 530 melting point apparatus. ^1H NMR and ^{13}C NMR spectra were recorded using Bruker 250 MHz or Varian 500 MHz. Chemical shifts were given in parts per million and coupling constants (*J*) in hertz. Mass spectra were obtained using a JMS-HX 110A/110A Tandem Mass Spectrometer (JEOL). UV absorption spectra were obtained on UVIKON 933 Double Beam UV/VIS Spectrometer. Fluorescence emission spectra were obtained using RF-5301/PC Spectrofluorophotometer (Shimadzu).

4.1.1. 1,1'-[9,10-Anthracenediylbis(methylene)]bis[3-butyl-1*H*-imidazolium] dihexafluorophosphate (3**). *Procedure A.* A solution of 9,10-bis(bromomethyl)anthracene^{4a} **10** (100 mg, 0.27 mmol) and 1-butylimidazole (70 mg, 0.56 mmol) in acetonitrile (25 mL) was refluxed for 12 h. After cooling to the room temperature, the solvent was evaporated to dryness under vacuum. To the reaction mixture, 10 mL of acetone was added. After stirring for 20 min at room temperature, 109 mg of KPF₆ (0.54 mmol) was added to the reaction mixture. After another 24 h stirring at room temperature, the reaction mixture was filtered and the filtrate was evaporated. To the oily crude product, about 5 mL of ethyl acetate was added. The addition of ethyl acetate caused the precipitation of the product. The precipitate was then filtered and washed with CH_2Cl_2 to give analytically pure product as a pale yellow solid (160 mg, 80%); mp 248–252 °C, dec; ^1H NMR (CD_3CN) δ 8.39 (m, 4H), 8.26 (s, 2H), 7.75 (m, 4H), 7.36 (m, 4H), 6.39 (s, 4H), 3.99 (t, 4H, *J*=7.4 Hz), 1.71 (quintet, 4H, *J*=7.3 Hz), 1.20 (sextet, 4H, *J*=7.3 Hz), 0.86 (t, 6H, *J*=7.4 Hz); ^{13}C NMR (CD_3CN) δ 135.6, 131.4, 128.4, 126.6, 124.6, 122.9, 122.8, 49.9, 146.1, 31.8, 19.3, 12.9; MS (FAB) *m/z*=597.2587 ($\text{M}-\text{PF}_6$)⁺, calcd for $[\text{C}_{30}\text{H}_{36}\text{F}_{12}\text{N}_4\text{P}_2-\text{PF}_6]=597.2582$.**

4.1.2. (S)-(-)-2,2'-Bis[(*n*-butyl)imidazoliummethyl]-1,1'-binaphthyl dihexafluorophosphate (4**). Application of procedure A to (S)-(-)-2,2'-bis(bromomethyl)-1,1'-binaphthyl **11**¹² (80 mg, 0.18 mmol) and 1-butylimidazole (70 mg, 0.56 mmol) in acetonitrile (25 mL) gave **4** as an analytically pure solid (129 mg, 76%); mp 166–170 °C, dec; ^1H NMR ($\text{DMSO}-d_6$, 250 MHz) δ 8.54 (s, 1H), 8.26 (d, 2H, *J*=8.5 Hz), 8.08 (d, 2H, *J*=8.5 Hz), 7.79 (d, 2H, *J*=8.5 Hz), 7.51 (t, 2H, *J*=7.2 Hz), 7.36 (br s, 2H), 7.19 (t, 2H,**

$J=7.2$ Hz), 7.41 (t, 2H, $J=1.8$ Hz), 7.15 (br s, 2H), 6.63 (d, 2H, $J=8.4$ Hz), 5.33 (d, 2H, $J=15.0$ Hz), 5.11 (d, 2H, $J=15.0$ Hz), 3.38 (m, 4H), 1.50 (quintet, 4H, $J=7.3$ Hz), 1.14 (sextet, 4H, $J=7.3$ Hz), 0.83 (t, 6H, $J=7.3$ Hz); ^{13}C NMR (DMSO- d_6 , 125 MHz) δ 135.7, 133.9, 132.9, 131.8, 130.2, 129.6, 128.2, 127.6, 127.0, 126.9, 124.9, 122.4, 121.9, 51.1, 48.3, 31.0, 18.7, 13.2; HRMS (FAB) $m/z=673.2894$ ($\text{M}-\text{PF}_6$) $^+$, calcd for $[\text{C}_{36}\text{H}_{40}\text{F}_{12}\text{N}_4\text{P}_2-\text{PF}_6]=673.2895$.

4.2. Preparation of fluorometric anion titration solutions

Stock solutions (1 mM) of the tetrabutylammonium salts of $\text{HP}_2\text{O}_7^{3-}$, H_2PO_4^- , HSO_4^- , CH_3CO_2^- , F^- , Cl^- , Br^- , and I^- in acetonitrile were prepared. Stock solutions of **1–9** (0.1 mM) were also prepared either in acetonitrile or DMSO. Test solutions were prepared by placing 4–40 μL of the probe stock solution into a test tube, adding an appropriate aliquot of each metal stock, and diluting the solution to 4 mL with acetonitrile. For all measurements, excitation was at 365 nm (for **1**, **2**, **3**), 310 nm (for **4**), 272 nm (for **5**) or 320 nm (for **6–9**); emission was measured at 421 nm (for **1** and **3**), 418 nm (for **2**) or 342 nm (for **4**). Both excitation and emission slit widths were 3 nm or 5 nm.

4.3. Preparation of NMR-titration solutions

The solution of receptors as 1 mM in CD_3CN was titrated by adding known quantities of concentrated solution (4 mM) of anions in the form of their tetrabutylammonium salts. All tetrabutylammonium anions were purchased from Aldrich. All titrations were repeated at least once to get the consistent values.

4.4. X-ray structure determination

The X-ray diffraction data for suitable crystals were collected and mounted on a Bruker-SMART-CCD-2000-APEX diffractometer with monochromated Mo $K\alpha$ radiation ($\lambda=0.71069$ Å) in the $\omega/2\theta$ scan and measured. The SHELX programs were used for structure solution and refinement.¹⁹

4.4.1. Compound 3·2(PF₆). $\text{C}_{30}\text{H}_{36}\text{F}_{12}\text{N}_4\text{P}_2$; the data crystal is in a colorless plate form and had approximate dimensions $0.1 \times 0.1 \times 0.05$ mm³, orthorhombic, space group $Pbca$, $a=12.731(4)$ Å, $b=10.549(3)$ Å, $c=24.840(8)$ Å; $V=3336.0(2)$ Å³, $Z=4$, $F(000)=1528$, $\sigma=1.478$ Mg/m³, $2\theta_{\text{max}}=49.46^\circ$, $R1=0.0735$, $wR2=0.1739$, $\text{GOF}=1.001$, residual electron density between 0.403 and -0.196 e Å⁻³. Crystallographic data for the structure (**3·2(PF₆)**) have been deposited to the Cambridge Crystallographic Data Centre as supplementary publication no. CCDC-275816. These data can be obtained free of the charge from the Cambridge Crystallographic Data Centre via www.ccdc.cam.ac.uk/_conts/retrieving.html.

Acknowledgements

This work was supported by the Korea Research Foundation Grant (KRF-R14-2003-014-01001-0 and KRF-2004-005-C00093), the Creative Research Initiative of the Korean Ministry of Science and Technology, and BK21.

References and notes

- For recent reviews for anion receptors, see: (a) Sessler, J. L.; Seidel, D. *Angew. Chem., Int. Ed.* **2003**, *42*, 5134; (b) Beer, P. D.; Gale, P. A. *Angew. Chem., Int. Ed.* **2001**, *40*, 486; (c) Snowden, T. S.; Anslyn, E. V. *Chem. Biol.* **1999**, *3*, 740; (d) Antonisse, M. M. G.; Reinhoudt, D. N. *Chem. Commun.* **1998**, 143; (e) Schmidtchen, F. P.; Berger, M. *Chem. Rev.* **1997**, *97*, 1609; (f) Rudkevich, D. M.; Brzozka, Z.; Palys, M.; Visser, H. C.; Verboom, W.; Reinhoudt, D. N. *Angew. Chem., Int. Ed. Engl.* **1994**, *33*, 467; (g) Martínez-Mañez, R.; Sancañón, F. *Chem. Rev.* **2003**, *103*, 4419.
- (a) *Fluorescent Chemosensors for Ion and Molecular Recognition*; Czarnik, A. W., Ed.; American Chemical Society: Washington, DC, 1993; (b) Czarnik, A. W. *Acc. Chem. Res.* **1994**, *27*, 302; (c) Fabbrizzi, L.; Poggi, A. *Chem. Soc. Rev.* **1994**, *197*; (d) de Silva, A. P.; Gunaratne, H. Q. N.; Gunlaugsson, T. A.; Huxley, T. M.; McCoy, C. P.; Rademacher, J. T.; Rice, T. E. *Chem. Rev.* **1997**, *97*, 1515; (e) *Chemosensors of Ion and Molecular Recognition*; Desvergne, J.-P., Czarnik, A. W., Eds.; Kluwer Academic: Dordrecht, The Netherlands, 1997; (f) Callan, J. F.; de Silva, A. P.; Magri, D. C. *Tetrahedron* **2005**, *61*, 8551.
- Mathews, C. P.; van Hold, K. E. *Biochemistry*; The Benjamin/Cummings: Redwood City, CA, 1990.
- (a) Kim, S. K.; Singh, N. J.; Kim, S. J.; Swamy, K. M. K.; Kim, S. H.; Lee, K.-H.; Kim, K. S.; Yoon, J. *Tetrahedron* **2005**, *61*, 4545; (b) Lee, D. H.; Kim, S. Y.; Hong, J.-I. *Angew. Chem., Int. Ed.* **2004**, *43*, 4777; (c) Gunlaugsson, T.; Davis, A. P.; O'Brien, J. E.; Glynn, M. *Org. Lett.* **2002**, *4*, 2449; (d) Fabbrizzi, L.; Marcotte, N.; Stomeo, F.; Taglietti, A. *Angew. Chem., Int. Ed.* **2002**, *41*, 3811; (e) Anzenbacher, P., Jr.; Jursíková, K.; Sessler, J. L. *J. Am. Chem. Soc.* **2000**, *122*, 9350; (f) Nishizawa, S.; Kato, Y.; Teramae, N. *J. Am. Chem. Soc.* **1999**, *121*, 9463; (g) Vance, D. H.; Czarnik, A. W. *J. Am. Chem. Soc.* **1994**, *116*, 9397.
- Yoon, J.; Kim, S. K.; Singh, N. J.; Kim, K. S., *Chem. Soc. Rev.* **2006**, *35*, 355.
- (a) Yun, S.; Ihm, H.; Kim, H. G.; Lee, C.; Indrajit, W. B.; Oh, K. S.; Gong, Y. J.; Lee, J. W.; Yoon, J.; Lee, H. C.; Kim, K. S. *J. Org. Chem.* **2003**, *68*, 2467; (b) Ihm, H.; Yun, S.; Kim, H. G.; Kim, J. K.; Kim, K. S. *Org. Lett.* **2002**, *4*, 2897; (c) Yuan, Y.; Jiang, Z.-L.; Yan, J.-M.; Gao, G.; Chan, A. S. C.; Xie, R.-G. *Synth. Commun.* **2000**, *30*, 4555; (d) Sato, K.; Arai, S.; Yamagishi, T. *Tetrahedron Lett.* **1999**, *40*, 5219.
- (a) Baker, M. V.; Bosnich, M. J.; Brown, D. H.; Byrne, L. H.; Hesler, V. J.; Skelton, B. W.; White, A. H.; Williams, C. C. *J. Org. Chem.* **2004**, *69*, 7640; (b) Sato, K.; Onitake, T.; Arai, S.; Yamagishi, T. *Heterocycles* **2003**, *60*, 779; (c) Yuan, Y.; Gao, G.; Jiang, Z.-L.; You, J.-S.; Zhou, Z.-Y.; Yuan, D.-Q.; Xie, R.-G. *Tetrahedron* **2002**, *58*, 8993; (d) Ramos, S.; Alcade, E.; Doddi, G.; Mencarelli, P.; Pérez-García, L. *J. Org. Chem.* **2002**, *67*, 8463; (e) Rajakumar, P.; Dhanasekaran, M. *Tetrahedron* **2002**, *58*, 1355; (f) Bitter, I.; Török, Z.; Csokai, V.; Grün, A.; Balázs, B.; Tóth, G.; Keserü, G. M.; Kovári, Z.; Czugler, M. *Eur. J. Org. Chem.* **2001**, 2861; (g) Alcade, E.; Alvarez-Rúa, C.; García-Rodríguez, E.; Mesquida, N.; Pérez-García, L. *Chem. Commun.* **1999**, 295; (h) Rajakumar, P.; Srisailas, M. *Tetrahedron Lett.* **1997**, *38*, 5323.
- Chellappan, K.; Singh, N. J.; Hwang, I.-C.; Lee, J. W.; Kim, K. S. *Angew. Chem., Int. Ed.* **2005**, *44*, 2899.
- (a) Kwon, J. Y.; Singh, N. J.; Kim, H.; Kim, S. K.; Kim, K. S.; Yoon, J. *J. Am. Chem. Soc.* **2004**, *126*, 8892; (b) Yoon, J.;

- Kim, S. K.; Singh, N. J.; Lee, J. W.; Yang, Y. J.; Chellappan, K.; Kim, K. S. *J. Org. Chem.* **2004**, *69*, 581; (c) Kim, S. K.; Singh, N. J.; Kim, S. J.; Kim, H. G.; Kim, J. K.; Lee, J. W.; Kim, K. S.; Yoon, J. *Org. Lett.* **2003**, *5*, 2083.
10. Frank, M.; Maas, G.; Schatz, J. *Eur. J. Org. Chem.* **2004**, 607.
11. (a) Kim, S. K.; Kang, B.-G.; Koh, H. S.; Yoon, Y.-J.; Jung, S. J.; Jeong, B.; Lee, K.-D.; Yoon, J. *Org. Lett.* **2004**, *6*, 4655; (b) Kim, S. K.; Moon, B.-S.; Park, J. H.; Seo, Y. I.; Koh, H. S.; Yoon, Y. J.; Lee, K.-D.; Yoon, J. *Tetrahedron Lett.* **2005**, *46*, 6617.
12. Ho, H. A.; Leclerc, M. *J. Am. Chem. Soc.* **2003**, *125*, 4412.
13. (a) Hayashi, T.; Hayashizake, K.; Takao, K.; Ito, Y. *J. Am. Chem. Soc.* **1988**, *110*, 8153; (b) Colletti, S. L.; Halterman, R. L. *Tetrahedron Lett.* **1989**, *30*, 3513.
14. (a) Connors, K. A. *Binding Constants*; Wiley: New York, NY, 1987; (b) Association constants were obtained using the computer program ENZFITTER, available from Elsevier-BIOSOFT, 68 Hills Road, Cambridge CB2 1LA, United Kingdom.
15. (a) Bai, Y.; Zhang, B.-G.; Xu, J.; Duan, C.-Y.; Dang, D.-B.; Liu, D.-J.; Meng, Q.-J. *New J. Chem.* **2005**, *29*, 777; (b) Vickers, M. S.; Martindale, K. S.; Beer, P. D. *J. Mater. Chem.* **2005**, *15*, 2784; (c) Kim, H.; Kang, J. *Tetrahedron Lett.* **2005**, *46*, 5443.
16. Tobey, S. L.; Anslyn, E. V. *J. Am. Chem. Soc.* **2003**, *125*, 10963.
17. Density functional calculations (B3LYP/6-31(+)G*) and self-consistent-reaction field (SCRF) calculations (solvent: acetonitrile; dielectric constant: 36.6) were carried out. Kim, K. S.; Tarakeshwar, P.; Lee, J. Y. *Chem. Rev.* **2000**, *100*, 4145.
18. (a) Singh, N. J.; Olleta, A. C.; Kumar, A.; Park, M.; Yi, H.-B.; Bandyopadhyay, I.; Lee, H. M.; Tarakeshwar, P.; Kim, K. S. *Theor. Chem. Acc.* **2006**, *115*, 127; (b) Lee, H. M.; Kim, D.; Kim, K. S. *J. Chem. Phys.* **2002**, *116*, 5509; (c) Lee, H. M.; Kim, K. S. *J. Chem. Phys.* **2001**, *114*, 4461; (d) Kim, J.; Lee, H. M.; Suh, S. B.; Majumdar, D.; Kim, K. S. *J. Chem. Phys.* **2000**, *113*, 5259; (e) Majumdar, D.; Kim, J.; Kim, K. S. *J. Chem. Phys.* **2000**, *112*, 101.
19. (a) *SMART V 5.6 Software for the CCD Detector System*; Bruker APEX II: Madison, WI, 2000; (b) Sheldrick, G. M. *SHELXTL V 6.1, Program for Crystal Structure Refinement*, Universität Göttingen, 1997.